Two-Timescale Design for Uplink Systems: How Many IRS Beamforming Patterns Are Needed?

Guangji Chen, Qingqing Wu, and Wen Chen, *Senior Member, IEEE*

***Abstract*—In this article, we develop a new dynamic intelligent reflecting surface (IRS) beamforming (BF) framework for an IRS aided energy-constrained Internet-of-Things system, where multiple IRS BF patterns are employed to assist uplink transmission. To alleviate the channel estimation overhead incurred by the IRS, a novel two-timescale scheme is proposed to maximize the ergodic sum-rate. Specifically, multiple IRS BF patterns are first optimized based on the statistical channel state information (CSI). Under the obtained IRS BF patterns, the transmit power and time allocation for devices in each channel coherence interval are optimized based on the instantaneous CSI. By characterizing the lower bound of the objective value, we further analytically quantify the performance degradation incurred by using less IRS BF patterns to shed light on the fundamental performance-overhead tradeoff. Simulation results validate the effectiveness of our proposed design and demonstrate that only 33% of the total IRS BF patterns are needed to maintain 95% of the maximum achieved ergodic sum-rate.**

***Index Terms*—IRS, statistical CSI, dynamic beamforming.**

I. Introduction

Intelligent reflecting surface (IRS) has recently emerged as a innovative technology to enhance the spectral- and energy-efficiency of future wireless networks cost-effectively, by smartly adjusting the phase shifts of a large number of low-cost reflecting elements [1]. Particularly, the seminal work [2] unveiled that the fundamental squared power gain of the IRS can be reaped even with the discrete phase shifts. Such a promising power scaling law has motivated an intensive research interests on integrating IRS in various applications (see [3] and the references therein).

One unique feature for the IRS is that its phase shifts can be reconfigured multiple times in a channel coherence interval to create favorable time-selective channels, which gives rise to a novel technique called dynamic IRS beamforming (DIBF) [4], [5], [6], [7], [8], [9]. Multiple IRS beamforming (BF) patterns introduced by the DIBF offer new degrees-of-freedom (DoF) to further enhance the multiuser diversity over time and thus enables more flexible resource allocation. By considering the interplay between DIBF and multiple access (MA) schemes, the minimum transmit powers required by different MA schemes were analyzed under the two-user case [4]. The capacity region for different MA schemes in a general multiuser setup was further characterized in [5] by considering the effect of DIBF. The concept of DIBF is also practically appealing in various Internet-of-Things (IoT) scenarios to make use of multiple IRS BF patterns for improving the data uploading efficiency, such as wireless powered communication networks (WPCNs) [6], [7] and mobile edge computing (MEC) [8], [9]. In particular, the authors in [7] proposed a novel and unified optimization framework for DIBF to maximize the system sum throughput.

Manuscript received 10 July 2022; revised 3 October 2022; accepted 6 November 2022. Date of publication 15 November 2022; date of current version 18 April 2023. This work was supported by the FDCT under Grant 0119/2020/A3 and in part by National key project under Grant 2020YFB1807700 and Grant 2018YFB1801102, in part by Shanghai Kewei under Grant 20JC1416502 and Grant 22JC1404000, in part by Pudong under Grant PKX2021-D02 and in part by NSFC under Grant 62071296. The review of this article was coordinated by Prof. Jingon Joung. *(Corresponding author: Qingqing Wu.)*

Guangji Chen is with the State Key Laboratory of Internet of Things for Smart City, University of Macau, Macao 999078, China (e-mail: guangjichen@um.edu.mo).

Qingqing Wu and Wen Chen are with the Department of Electronic Engineering, Shanghai Jiao Tong University, Shanghai 200240, China (e-mail: wu.qq1010@gmail.com; wenchen@sjtu.edu.cn).

Digital Object Identifier 10.1109/TVT.2022.3222339

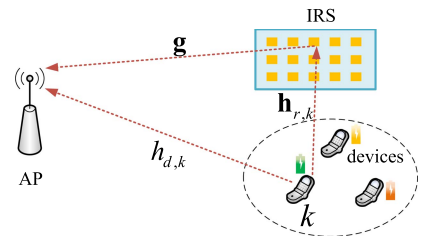

Fig. 1. An IRS-aided energy-constrained uplink communication system.

It is worth pointing out that all the aforementioned works on the IRS BF design are based on the instantaneous channel state information (I-CSI) for all the IRS-associated links. To obtain such CSI in a channel coherence interval, its associated channel estimation overhead scales with the number of IRS elements and users. To overcome this issue, [10], [11], [12], [13] proposed two-timescale based IRS BF designs relying on the statistical CSI (S-CSI), which greatly reduces the channel estimation overhead. However, the IRS BF was assumed to remain static throughout the whole channel coherence interval in [10], [11], [12], [13], which thus underestimates the potential gain of the IRS in practice.

Different from [10], [11], [12], [13], this paper focuses on exploiting multiple IRS BF patterns to assist uplink transmission from multiple energy-constrained IoT devices to an access point (AP), as shown in Fig. 1. Due to the limited computing capability of the IRS, the IRS BF patterns are usually computed at the AP and then are fed back from the AP to the IRS controller for reconfiguring reflection [2], [7]. Thus, the resulting feedback overhead increases linearly with the number of IRS BF patterns and reflecting elements. In the case with massive IoT devices and IRS reflecting elements, both the huge channel estimation overhead and feedback overhead may become practically unaffordable, which leads to the following two fundamental issues to be addressed. First, how to design an efficient protocol to reduce the requirement for the large amount of the I-CSI? Second, how to determine the number of IRS BF patterns employed in each channel coherence interval to balance the performance and its associated feedback overhead?

Motivated by the above considerations, we propose in this paper a novel two-timescale protocol to maximize the ergodic sum-rate. First, we derive a tractable upper bound for the ergodic sum-rate, based on which, multiple IRS BF patterns are optimized in the large timescale relying on the S-CSI. Then, in each channel coherence interval, the transmit power and time allocation of each device are optimized based on the effective I-CSI under the IRS BF patterns obtained in the first step. Since the dimension of the effective I-CSI is independent of the number of IRS elements, the corresponding channel estimation overhead can be significantly reduced. To further balance the system performance and its associated feedback overhead, we theoretically characterize the relationship between the objective value and the number of IRS BF patterns. The performance degradation incurred by adopting less IRS BF patterns compared to the maximum achievable sum-rate is analytically quantified, which sheds light on the

0018-9545 © 2022 IEEE. Personal use is permitted, but republication/redistribution requires IEEE permission.
See https://www.ieee.org/publications/rights/index.html for more information.

Authorized licensed use limited to: Shanghai Jiaotong University. Downloaded on June 05,2023 at 08:45:12 UTC from IEEE Xplore. Restrictions apply.

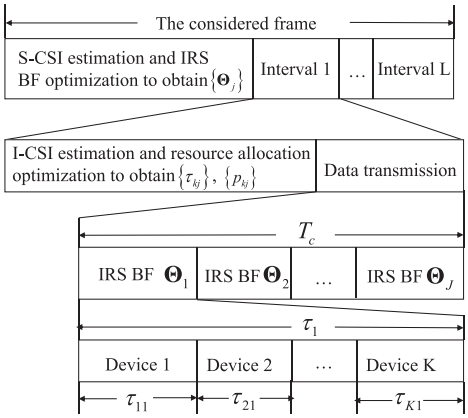

Fig. 2. Illustration of the two-timescale based transmission protocol with DIBF.

minimum IRS BF patterns required for guaranteeing a certain level of performance. Simulation results validate our theoretical analysis and show that the proposed design is able to achieve 95% of the maximum sum-rate with only $K/3$ IRS BF patters, where K denotes the required IRS BF patterns for obtaining the maximum system sum-rate.

II. System Model and Problem Formulation

As shown in Fig. 1, we consider a typical IRS-aided energy-constrained uplink communication system, where K single-antenna IoT devices transmit data to a single-antenna AP with the aid of an IRS equipped with N reflecting elements. Note that it can be readily extended to the case with multiple antennas at the AP by incorporating the active beamforming design at the AP [2]. The equivalent baseband channels from the IRS to the AP, from device k to the IRS, and from device k to the AP are denoted by $\mathbf{g} \in \mathbb{C}^{N\times 1}$, $\mathbf{h}_{r,k} \in \mathbb{C}^{N\times 1}$, and $h_{d,k} \in \mathbb{C}$, respectively, where $k = 1, \ldots, K$. Without loss of generality, we adopt the Rician fading model as in [11], [12], [13] to characterize the device k-IRS link and IRS-AP link as

$$\mathbf{h}_{r,k} = \rho_{r,k}\left(\sqrt{\gamma_k/(\gamma_k+1)}\bar{\mathbf{h}}_{r,k} + \sqrt{1/(\gamma_k+1)}\tilde{\mathbf{h}}_{r,k}\right), \quad (1)$$

$$\mathbf{g} = \rho_g\left(\sqrt{\gamma_g/(\gamma_g+1)}\bar{\mathbf{g}} + \sqrt{1/(\gamma_g+1)}\tilde{\mathbf{g}}\right), \quad (2)$$

where $\rho_{r,k}^2$ and ρ_g^2 are distance-based large-scale path-loss, γ_k and γ_g are Rician factors. $\bar{\mathbf{h}}_{r,k}$ and $\bar{\mathbf{g}}$ are deterministic line-of-sight (LoS) channel components. By contrast, $\tilde{\mathbf{h}}_{r,k}$ and $\tilde{\mathbf{g}}$ are non-LoS (NLoS) channel components, whose elements are independent and identical distribution random variables following $\mathcal{CN}(0,1)$. Note that rich scatters often exist near the ground. As in previous works [12], [13], we adopt the Rayleigh fading model to characterize the direct links between devices and the AP. The channel of direct links can be rewritten as $h_{d,k} = \rho_{d,k}\tilde{h}_{d,k}$, where $\rho_{d,k}^2$ denotes the large-scale path loss and $\tilde{h}_{d,k} \sim \mathcal{CN}(0,1)$. In this paper, $\{\bar{\mathbf{h}}_{r,k}, \bar{\mathbf{g}}\}$ refers to S-CSI and $\{\tilde{\mathbf{h}}_{r,k}, \tilde{\mathbf{g}}, \tilde{h}_{d,k}\}$ refers to I-CSI, respectively.

To alleviate the channel estimation incurred by massive devices and reflecting elements, we introduce the proposed two-timescale based transmission protocol with DIBF. As shown in Fig. 2, we focus on a frame in which the S-CSI of all links is assumed to remain static. At the beginning of the considered frame, the S-CSI is acquired firstly and then a total number of J ($J \geq 1$) IRS BF patterns are optimized based on the S-CSI. Note that the considered frame consists of multiple channel coherence intervals and the I-CSI is assumed to be constant in each channel coherence interval. The time duration for data transmission in a channel coherence interval is denoted by T_c. In each channel coherence interval, the obtained J IRS BF patterns are sequentially employed over time for assisting data transmission of devices, each of which is denoted by $\mathbf{\Theta}_j = \mathrm{diag}(e^{i\theta_{j,1}}, \ldots, e^{i\theta_{j,N}})$ with $\theta_{j,n} \in [0, 2\pi)$, $j = 1, \ldots, J, n = 1, \ldots, N$. Note that $\{\mathbf{\Theta}_j\}$ is designed based on the S-CSI and remains constant in the considered frame, which will be discussed latter. The data transmission stage of each channel coherence interval is divided into J time slots (TSs) and the time duration for the j-th TS is denoted by τ_j, in which $\mathbf{\Theta}_j$ is employed. Each TS, τ_j, is further partitioned into K sub-TSs and the time duration for the k-th sub-TS is denoted by τ_{kj}, where device k would transmit its signal to the AP. Accordingly, the achievable rate of device k in a channel coherence interval is given by

$$R_k = \sum_{j=1}^{J} \tau_{kj}\log_2\left(1 + \frac{p_{kj}g_{kj}}{\sigma^2}\right), \quad (3)$$

where $g_{kj} = |h_{kj}|^2$ with $h_{kj} = h_{d,k} + \mathbf{h}_{r,k}^H\mathbf{\Theta}_j\mathbf{g}$ and p_{kj} denotes the transmit power of device k when employing $\mathbf{\Theta}_j$. In each time coherence interval with any given $\{\mathbf{\Theta}_j\}$, the resource allocation with respect to $\{p_{kj}, \tau_{kj}\}$ is optimized based on the effective I-CSI, i.e., $\{h_{kj}\}$.

We aim to maximize the ergodic sum-rate of all the devices by jointly optimizing the short-term resource allocation $\{p_{kj}, \tau_{kj}\}$ and the long-term IRS BF patterns $\{\mathbf{\Theta}_j\}$. The corresponding optimization problem can be written as

$$\max_{\{\mathbf{\Theta}_j\}} \ \mathbb{E}\left\{\max_{\{p_{kj}\},\{\tau_{kj}\}} \sum_{k=1}^{K} R_k\right\} \quad (4a)$$

$$\text{s.t.} \ \sum_{j=1}^{J} \tau_{kj}p_{kj} \leq E_{\max}, \forall k, \quad (4b)$$

$$\sum_{k=1}^{K}\sum_{j=1}^{J} \tau_{kj} \leq T_c, \quad (4c)$$

$$\tau_{kj} \geq 0, \ p_{kj} \geq 0, \ \forall k, j, \quad (4d)$$

$$\left|[\mathbf{\Theta}_j]_{n,n}\right| = 1, \forall j, n. \quad (4e)$$

In problem (4), the inner sum-rate maximization problem is over the short-term resource allocation in each channel coherence interval for the given IRS BF patterns $\{\mathbf{\Theta}_j\}$, while the outer rate-maximization problem is over the long term IRS BF patterns, where the expectation is taken over all I-CSI's random realization within the considered frame. Constraint (4b) ensures that the total energy consumed at each device cannot exceed its energy budget, denoted by $E_{\max}$. Constraints (4c) and (4d) are the total transmission time constraint and the non-negative constraints on the optimization variables, respectively, while (4e) is the unit-modulus constraint for each IRS BF pattern.

Remark 1: Regarding our proposed DIBF based two-timescale protocol, the IRS BF patterns are obtained based on the S-CSI and remain static in a frame. As such, in each channel coherence interval, only the effective I-CSI, i.e., $\{h_{kj}\}$, needs to be estimated for optimizing $\{p_{kj}\}, \{\tau_{kj}\}$. The channel training overhead in each channel coherence interval is independent of N and thus can be significantly reduced compared to previous works [6], [7], [8], [9]. Moreover, the feedback information of IRS BF patterns from the AP to the IRS controller is JN. By controlling J, a flexible tradeoff between the DoF to adjust the IRS BF and its associated feedback signalling overhead can be achieved.

Authorized licensed use limited to: Shanghai Jiaotong University. Downloaded on June 05,2023 at 08:45:12 UTC from IEEE Xplore. Restrictions apply.

III. Proposed Solution and Performance Analysis

Problem (4) is challenging to solve because 1) the short-term optimization variables $\{\tau_{kj}, p_{kj}\}$ and long-term IRS BF patterns $\{\mathbf{\Theta}_j\}$ are intricately coupled in the objective function (4a); 2) a closed-form expression of the ergodic sum-rate under the optimized $\{\tau_{kj}, p_{kj}\}$ and any given $\{\mathbf{\Theta}_j\}$ is difficult to obtain in general. To overcome these challenges, we propose an efficient algorithm to solve problem (4) and characterize the lower bound of the objective value with respect to J in the next two subsections, respectively.

A. Proposed Solution

In this subsection, we propose a two-step approach to solve problem (4). Specifically, the closed-form expression for the ergodic sum-rate is derived by deeply exploiting the inherent structure of (4). Based on the closed-form expression, $\{\mathbf{\Theta}_j\}$ is obtained by employing the successive convex approximation (SCA) technique. Then, $\{p_{kj}, \tau_{kj}\}$ in each channel coherence interval is optimized under the obtained $\{\mathbf{\Theta}_j\}$. To proceed, we first present the following lemma to simplify problem (4).

Lemma 1: For arbitrarily given IRS BF patterns $\{\mathbf{\Theta}_j\}$, the optimal $\{\tau_{kj}, p_{kj}\}$ for problem (4) satisfies

$$\tau_{k\Omega(k)} > 0, \tau_{kj} = 0\,(j \neq \Omega(k)), \sum_{k=1}^{K} \tau_{k\Omega(k)} \leq T_c, \tag{5}$$

$$p_{k\Omega(k)} = E_{\max}/\tau_{k\Omega(k)}, p_{kj} = 0\,(j \neq \Omega(k)), \tag{6}$$

where $\Omega(k) = \arg\max_{j\in\{1,\ldots,J\}} |h_{d,k} + \mathbf{h}_{r,k}^H \mathbf{\Theta}_j \mathbf{g}|^2, \forall k$.

Proof: The main procedures are similar to [7]. Interested readers may refer to [7] for more details.

By exploiting Lemma 1, R_k can be rewritten as

$$\tilde{R}_k = \tau_{\Omega(k)} \log_2 \left(1 + \frac{E_{\max}\left|h_{d,k} + \mathbf{h}_{r,k}^H \mathbf{\Theta}_{\Omega(k)} \mathbf{g}\right|^2}{\tau_{\Omega(k)}\sigma^2}\right) \tag{7}$$

Thus, problem (4) can be further simplified as an equivalent form as follows

$$\max_{\{\mathbf{\Theta}_j\}} \ \mathbb{E}\left\{\max_{\{\tau_{k\Omega(k)}\},\{\Omega(k)\}} \sum_{k=1}^{K} \tilde{R}_k\right\} \tag{8a}$$

$$\text{s.t.} \ \sum_{k=1}^{K} \tau_{k\Omega(k)} \leq T_c, \tag{8b}$$

$$\tau_{k\Omega(k)} \geq 0, (4e). \tag{8c}$$

Based on the inner sum-rate maximization problem in (8), we provide an upper bound for the ergodic sum-rate in the following theorem.

Theorem 1: For any given $\{\mathbf{\Theta}_j\}$ and $\{\Omega(k)\}$, the ergodic sum-rate in (8a) is upper bounded by

$$\bar{R}^{ub}(J) = T_c \log_2 \left(1 + \frac{E_{\max}\sum_{k=1}^{K}\left(f_k\left(\mathbf{\Theta}_{\Omega(k)}\right) + C_k\right)}{T_c\sigma^2}\right), \tag{9}$$

where $f_k(\mathbf{\Theta}_{\Omega(k)}) = \beta_{1,k}\rho_{r,k}^2\rho_g^2|\bar{\mathbf{h}}_{r,k}^H \mathbf{\Theta}_{\Omega(k)}\bar{\mathbf{g}}|^2$ and $C_k = \beta_{2,k}\rho_{r,k}^2\rho_g^2 N + \rho_{d,k}^2$ with $\beta_{1,k} = \gamma_k\gamma_g/((\gamma_k+1)(\gamma_g+1))$ and $\beta_{2,k} = (\gamma_k+\gamma_g+1)/((\gamma_k+1)(\gamma_g+1))$.

Proof: Please refer to the Appendix A.

Note that Theorem 1 lays the foundation for optimizing $\{\mathbf{\Theta}_j\}$. It is observed that $\bar{R}^{ub}(J)$ in (9) does not depend on the I-CSI $\{\tilde{\mathbf{h}}_{r,k}, \tilde{\mathbf{g}}, \tilde{h}_{d,k}\}$, but only relies on the S-CSI $\{\bar{\mathbf{h}}_{r,k}, \bar{\mathbf{g}}\}$ and Rician factors $\{\gamma_g, \gamma_k\}$. Since the S-CSI changes much more slowly than the I-CSI, the optimization of IRS BF patterns based on the S-CSI only needs to be done for a relatively long time, which thus significantly reduces the CSI estimation overhead.

1) Optimization of $\{\mathbf{\Theta}_j\}$: Based on Theorem 1, the subproblem for maximizing $\bar{R}^{ub}(J)$ with respect to $\{\mathbf{\Theta}_j\}$ can be equivalently expressed as

$$\max_{\{\mathbf{\Theta}_j\},\{\Omega(k)\}} \sum_{k=1}^{K} f_k\left(\mathbf{\Theta}_{\Omega(k)}\right) \quad \text{s.t.} \ (4e). \tag{10}$$

For problem (10), it can be observed that at most K IRS BF patterns are sufficient to achieve the maximum ergodic sum-rate. When $J = K$, a dedicated IRS BF can be employed to maximize $f_k(\mathbf{\Theta}_{\Omega(k)}), \forall k$. In this case, $\Omega(k) = k$ and the optimal IRS BF patterns can be obtained as

$$[\mathbf{\Theta}_k^*]_{n,n} = e^{-i\arg\left(\left[\mathrm{diag}\left(\bar{\mathbf{h}}_{r,k}^H\right)\bar{\mathbf{g}}\right]_n\right)}, \forall k, n. \tag{11}$$

For the case of $J < K$, multiple devices may need to share the same IRS BF pattern. Note that both the optimal IRS BF patterns and their association relationship with devices, i.e., $\Omega(k)$, remain unknown. To address this issue, we propose an efficient scheme as follows. Specifically, we first sort all devices in descending order according to $f_k(\mathbf{\Theta}_{\Omega(k)})$. Without loss of generality, we assume that $f_1(\mathbf{\Theta}_1^*) \geq \cdots \geq f_K(\mathbf{\Theta}_K^*)$. Then, each of the first $J-1$ devices, i.e., $k = 1, \ldots J-1$, is assigned with a dedicated IRS BF pattern, i.e., $\mathbf{\Theta}_k = \mathbf{\Theta}_k^*, k = 1, \ldots J-1$. The remaining $K-J+1$ devices share the shame IRS BF pattern $\mathbf{\Theta}_J$. To obtain $\mathbf{\Theta}_J$, problem (10) can be transformed into

$$\max_{\{\mathbf{\Theta}_J\}} \sum_{k=J}^{K} f_k\left(\mathbf{\Theta}_J\right) \quad \text{s.t.} \ \left|[\mathbf{\Theta}_J]_{n,n}\right| = 1, \forall n. \tag{12}$$

Let $\mathbf{v}_J = [e^{i\theta_{J,1}}, \ldots, e^{i\theta_{J,N}}]^T$ and $\bar{\mathbf{q}}_k^H = \bar{\mathbf{h}}_{r,k}^H \mathrm{diag}(\bar{\mathbf{g}})$. Then, problem (12) can be equivalently rewritten as

$$\max_{\{\mathbf{v}_J\}} \sum_{k=J}^{K} w_k \left|\bar{\mathbf{q}}_k^H \mathbf{v}_J\right|^2 \quad \text{s.t.} \ \left|[\mathbf{v}_J]_n\right| = 1, \forall n, \tag{13}$$

where $w_k = \beta_{1,k}\rho_{r,k}^2\rho_g^2$. Although problem (13) is non-convex, the convexity of the objective function in (13) allows us to employ the SCA technique to solve it. Specifically, for a given local point $\hat{\mathbf{v}}_J$, a lower bound of the objective function in (13) can be obtained as

$$C_{\mathrm{lb}} = -\sum_{k=J}^{K} w_k \left|\bar{\mathbf{q}}_k^H \hat{\mathbf{v}}_J\right|^2 + 2\mathrm{Re}\left\{\hat{\mathbf{v}}_J^H \left(\sum_{k=J}^{K} w_k \bar{\mathbf{q}}_k \bar{\mathbf{q}}_k^H\right) \mathbf{v}_J\right\}. \tag{14}$$

The optimal solution for maximizing C_{lb} can be derived in closed-form as

$$\mathbf{v}_J = e^{j\arg\left(\left(\sum_{k=J}^{K} w_k \bar{\mathbf{q}}_k \bar{\mathbf{q}}_k^H\right)\hat{\mathbf{v}}_J\right)}. \tag{15}$$

By successively setting the IRS BF vector according to (15), the objective value of problem (13) will be non-decreasing over the iterations, where $\hat{\mathbf{v}}_J$ is obtained in the previous round of iterations. Moreover, the objective value of problem (13) is upper-bounded by a finite value, i.e.,

$$\sum_{k=J}^{K} w_k \left|\bar{\mathbf{q}}_k^H \mathbf{v}_J\right|^2 \overset{(a)}{\leq} \sum_{k=J}^{K} w_k N^2, \tag{16}$$

where (a) holds due to $|\bar{\mathbf{q}}_k^H \mathbf{v}_J|^2 \leq N^2$ for $\forall k \in \{J, \ldots, K\}$. Therefore, the proposed SCA-based algorithm for solving (13) is guaranteed to converge.

Authorized licensed use limited to: Shanghai Jiaotong University. Downloaded on June 05,2023 at 08:45:12 UTC from IEEE Xplore. Restrictions apply.

2) Optimization of $\{p_{kj}, \tau_{kj}\}$: Given the obtained $\{\mathbf{\Theta}_j\}$ in the previous subsection, the association relationship between each device and IRS BF patterns in each channel coherence interval can be determined as $\Omega(k) = \arg\max_{j\in\{1,\ldots,J\}} |h_{d,k} + \mathbf{h}_{r,k}^H \mathbf{\Theta}_j \mathbf{g}|^2, \forall k$. Then, the time allocation $\{\tau_{k\Omega(k)}\}$ can be obtained by solving the convex optimization problem as follows

$$\max_{\{\tau_{k\Omega(k)}\}} \sum_{k=1}^{K} \tilde{R}_k \quad \text{s.t. (8b)}, \ \tau_{k\Omega(k)} \geq 0, \forall k, \tag{17}$$

where $\tilde{R}_k$ is given in (7). Finally, the transmit power $\{p_{kj}\}$ is obtained based on (6) in Lemma 1.

Remark 2: The design principle in this paper is also applicable to the case with multiple antennas at the AP. To make such a extension, we assume that the AP is equipped with M antennas. Under this case, the channel from the device k to the AP and from the IRS to the AP are re-denoted by $\mathbf{h}_{d,k} \in \mathbb{C}^{M\times 1}$ and $\mathbf{G} \in \mathbb{C}^{M\times N}$, respectively. Regarding the two-timescale based transmission protocol, the IRS BF pattern is designed based on the S-CSI. Under the obtained IRS BF patterns $\{\mathbf{\Theta}_j\}$, the effective I-CSI, i.e., $\mathbf{h}_{d,k} + \mathbf{G}\mathbf{\Theta}_j \mathbf{h}_{r,k}$, is employed to jointly design the resource allocation and receive BF at the AP. The optimal receive BF vector is the maximum ratio combiner (MRC) [10] and can be expressed as $\mathbf{w}_{kj} = \mathbf{h}_{d,k} + \mathbf{G}\mathbf{\Theta}_j \mathbf{h}_{r,k}$. As such, the achievable rate of device k in a channel coherence interval is given by

$$R_k = \sum_{j=1}^{J} \tau_{kj} \log_2 \left(1 + \frac{p_{kj} \|\mathbf{h}_{d,k} + \mathbf{G}\mathbf{\Theta}_j \mathbf{h}_{r,k}\|^2}{\sigma^2}\right). \tag{18}$$

Following the similar steps in Appendix A, the closed-form expression of the ergodic sum-rate in this case can be easily derived. Then, the optimization approach to obtain $\{\mathbf{\Theta}_j\}$ and $\{p_{kj}, \tau_{kj}\}$ proposed in this section can be directly used to obtain those in the case with multiple antennas at the AP.

Remark 3: The design principle is applicable to the case by considering the correlation between the phase-shift and amplitude. As indicated by [14], there exists a coupling relationship between the reflection amplitude and phase shifts. Specifically, the IRS BF pattern employed in the j-th time slot is denoted by $\mathbf{\Theta}_j = \mathrm{diag}(v_{j,1}, \ldots, v_{j,N})$, where $v_{j,n} = a_{j,n}(\theta_{j,n}) e^{j\theta_{j,n}}$ with $\theta_{j,n} \in [0, 2\pi)$ and $a_{j,n}(\theta_{j,n}) \in [0, 1]$. The amplitude of the n-th element has the functional relationship with its phase-shift as follows

$$a_{j,n}(\theta_{j,n}) = (1 - a_{\min}) \left(\frac{\sin(\theta_{j,n} - \phi) + 1}{2}\right)^{\alpha} + a_{\min}, \tag{19}$$

where $a_{\min}$, ϕ, and α are the constants related to the specific circuit implementation [14]. It is evident that the proposed two-timescale based transmission protocol is still applicable to this case. The only difference is that the design of IRS beamforming patterns $\{\mathbf{\Theta}_j\}$ needs to re-consider constraint (19), which can be easily tackled by the element-wise alternating optimization or penalty-based method proposed in [14].

B. How Many IRS BF Patterns Do We Need?

In this subsection, we analytically quantify the performance loss incurred by using less IRS BF patterns. Under the optimal $\{\mathbf{\Theta}_j\}$, the corresponding optimal value for $\bar{R}^{ub}(J)$ in (9) is denoted by $\bar{R}^*(J)$. Then, we characterize the relationship between the ergodic sum-rate and the number of IRS BF patterns in the following proposition.

Proposition 1: Assuming that $f_1(\mathbf{\Theta}_1^*) \geq \cdots \geq f_K(\mathbf{\Theta}_K^*)$ without loss of generality, the lower bound of $\bar{R}^*(J)$ with J $(1 \leq J \leq K)$ IRS BF patterns is

$$\tilde{R}^{\mathrm{lb}}(J) = T_c \log_2 \left(1 + E_{\max} \left(\sum_{k=1}^{K} (C_k + G_K)\right) \Big/ \left(T_c \sigma^2\right)\right), \tag{20}$$

where $G_k = \beta_{1,k}\rho_{r,k}^2 \rho_g^2 N^2 (k \leq J)$, $G_k = f_k(\mathbf{\Theta}_J^*)(k > J)$, and $[\mathbf{\Theta}_J^*]_{n,n} = e^{-i\arg([\mathrm{diag}(\bar{\mathbf{h}}_{r,J}^H)\bar{\mathbf{g}}]_n)}, \forall n$.

Proof: One feasible solution for problem (10) can be constructed by letting the J IRS BF patterns, $\{\mathbf{\Theta}_j\}$, maximize $f_j(\mathbf{\Theta}_j), j = 1, \ldots J$, respectively. It can be easily verified that $\{\mathbf{\Theta}_j^*\}$ is one suboptimal solution for problem (10). Then, substituting them into (9) results in (20), which is the lower bound for the optimal value of $\bar{R}^{ub}(J)$ in (9).

For $\forall k \in \{J+1, \ldots, K\}$, $\beta_{1,k}\rho_{r,k}^2 \rho_g^2 N \geq f_k(\mathbf{\Theta}_J^*)$ always holds. As such, $\tilde{R}^{\mathrm{lb}}(J)$ is a non-decreasing function with respect to J. By setting $J = K$ and substituting $\{\mathbf{\Theta}_k^*\}$ into (9), the closed-form expression of the maximum achievable ergodic sum-rate can be obtained as

$$\bar{R}^{ub} = T_c \log_2 \left(1 + \frac{E_{\max} \sum_{k=1}^{K} \left(\beta_{1,k}\rho_{r,k}^2 \rho_g^2 N^2 + C_k\right)}{T_c \sigma^2}\right). \tag{21}$$

It can be verified that $\tilde{R}^{\mathrm{lb}}(K) = \bar{R}^{ub}$. Proposition 1 facilitates us to analyze the minimum number of IRS BF patterns required for maintaining a certain level of system performance. We denote ε as the ratio of the ergodic sum-rate with J IRS BF patterns to that with K BF patterns, i.e., $\varepsilon = \bar{R}^*(J)/\bar{R}^{ub}$. For the target ε_0, we reveal the required J for guaranteeing $\varepsilon \geq \varepsilon_0$ in the following proposition.

Proposition 2: $\varepsilon \geq \varepsilon_0$ always holds if $J \geq \tilde{J}$, where $\tilde{J}$ is the minimum integer for J which satisfies $\tilde{R}^{\mathrm{lb}}(J)/\bar{R}^{ub} \geq \varepsilon_0$.

Proof: Note that $\tilde{R}^{\mathrm{lb}}(J)$ is non-decreasing with respect to J and $\bar{R}^*(J) \geq \tilde{R}^{\mathrm{lb}}(J)$. For $\forall J \geq \tilde{J}$, we have

$$\bar{R}^*(J) \geq \tilde{R}^{\mathrm{lb}}(J) \geq \tilde{R}^{\mathrm{lb}}\left(\tilde{J}\right) \geq \varepsilon_0 \bar{R}^{ub}, \tag{22}$$

which thus completes the proof.

Proposition 2 provides an effective way to obtain the number of IRS BF patterns required for maintaining a certain portion of the maximum achievable sum-rate in an offline way. Since $\tilde{R}^{\mathrm{lb}}(J)$ is a non-decreasing function, $\tilde{J}$ can be efficiently obtained by applying bisection search between 1 and K.

IV. Numerical Results

In this section, we provide numerical results to examine the performance of our proposed design and draw useful insights. The AP and IRS are located at $(0, 0, 0)$ meter (m) and $(50, 0, 3)$ m, respectively. The devices are assumed to be randomly distributed within a radius of 10 m centered at $(50, 0, 0)$ m. The pathloss exponents of the AP-device links are set to 3.6, while those for both the AP-IRS and IRS-device links are set to 2.2. The signal attenuation at a reference distance of 1 m is set as 30 dB. Other system parameters are set as follows: $N = 100$, $E_{\max} = 0.01$ Joule, $\sigma^2 = -80$ dBm, and $T_c = 0.1$ s.

In Fig. 3, we show the ergodic sum-rate versus the number of IRS BF patterns under the different Rician factors, i.e., γ_k and γ_g. The designs based on the full I-CSI and random IRS BF are also considered for performance comparison. It can be observed that the performance of our proposed scheme significantly outperforms the random IRS BF and approaches that of the I-CSI-based design as the Rician factor increases since more statistical information can be exploited for optimizing the IRS BF patterns, which verifies the effectiveness of our proposed two-timescale design. To reduce the performance gap compared to the full

Authorized licensed use limited to: Shanghai Jiaotong University. Downloaded on June 05,2023 at 08:45:12 UTC from IEEE Xplore. Restrictions apply.

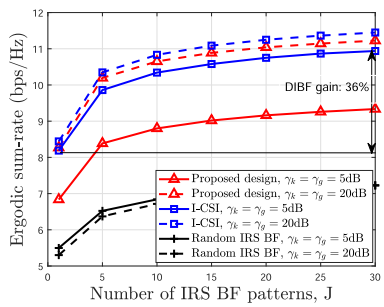

Fig. 3. Ergodic sum-rate versus the number of IRS BF petterns with $K = 30$.

TABLE I
PERFORMANCE LOSS INCURRED BY USING LESS IRS BF PATTERNS

J	1	5	10	15	20	30
ε	73.6%	91.4%	95.2%	97.1%	98.5%	100%

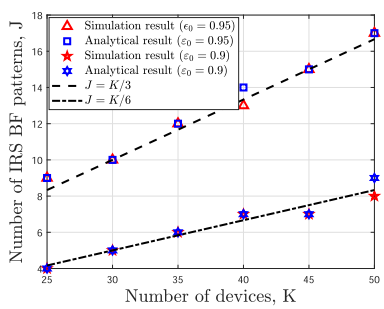

Fig. 4. Required J for $\bar{R}^*(J)/\bar{R}^{ub} \geq \varepsilon_0$ with $\gamma_g = \gamma_k = 5$ dB.

I-CSI-based desgin, the results imply the significance of deploying IRS to create LoS links with both the AP and devices. Moreover, one can observe that the sum-rate gain of $J = K$ over $J = 1$ is about 36% and the gain obtained by DIBF becomes gradually saturated as J increases.

To explicitly show the performance loss incurred by using less IRS BF patterns, we present $\varepsilon = \bar{R}^*(J)/\bar{R}^{lb}$ with respect to different J in Table 1 under the setup of $\gamma_k = \gamma_g = 5$ dB. From Table 1, the performance loss incurred by using less IRS BF patterns as compared to the upper-bound by using K IRS BF patterns becomes marginal when J is larger than a certain value. For example, using 10 IRS BF patters is practically sufficient to achieve close-to-optimal performance with slight performance loss (less than 5%). As such, one interesting question naturally arises: how many IRS BF patterns are needed to balance the performance-cost tradeoff?

To answer the above question, we plot the number of IRS BF patterns required for guaranteeing $\bar{R}^*(J)/\bar{R}^{ub} \geq \varepsilon_0$ versus K in Fig. 4, where "Simulation result" is obtained based on the sum-rate averaged over 1000 channel realizations and "Analytical result" is obtained based on Proposition 2. First, it can be verified that our analytical result in Proposition 2 provides a good approximation for the required J. As expected, the required J increases as K increases since more IRS BF patterns are required for supporting more devices to guarantee the system performance. Interestingly, it is observed that J/K remains at a nearly constant value regardless of the values of K, i.e., $1/3$ for $\varepsilon_0 = 0.95$ and $1/6$ for $\varepsilon_0 = 0.9$. The results reveal the fundamental tradeoff between the performance and associated signalling overhead, whereas they are promising by indicating that exploiting only $K/3$ IRS BF patterns is capable of achieving the near-optimal performance in practice.

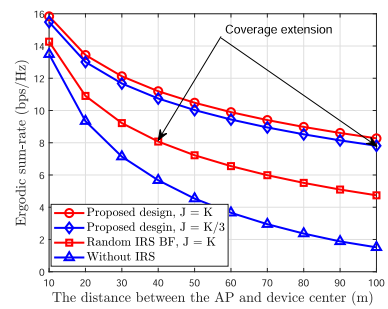

Fig. 5. Investigation of the coverage performance with $\gamma_g = \gamma_k = 5$ dB.

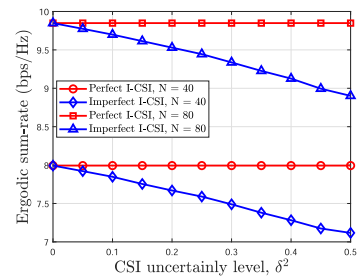

Fig. 6. Impact of imperfect I-CSI ($\gamma_k = \gamma_g = 5$ dB).

To verify the coverage performance of the proposed design, we plot the ergodic sum-rate versus the distance between the AP and the center of the device cluster in Fig. 5. Note that the location of the IRS is also adjusted accordingly to keep the relative distance with devices center unchanged. It is observed that the ergodic sum-rate of the proposed design decreases slowly than that of the scheme with random IRS beamforming and the system without IRS. For example, if the target ergodic sum-rate is set to 8 bps/Hz, devices with the distance beyond 40 m cannot meet the requirement in the case with random IRS beamforming or without IRS, whereas the requirement can be still met with 100 m under the proposed design.

Then, we further investigate the effect of imperfect I-CSI on the ergodic sum-rate. To capture the effect of imperfect I-CSI, we consider the CSI uncertainly model [15] as follows,

$$h_{kj} = \hat{h}_{kj} + e_{kj}, e_{kj} \sim \mathcal{CN}\left(0, \tilde{\delta}^2\right), \tag{23}$$

where $\hat{h}_{kj}$ and e_{kj} represent the estimated CSI and CSI estimation error, respectively. For this statistical CSI imperfection model, the variance of e_{kj} is defined as $\tilde{\delta}^2 = \delta^2|\hat{h}_{kj}|^2$, where $\delta^2 \in [0, 1)$ measures the relative amount of I-CSI uncertainty. In Fig. 6, we plot the ergodic sum-rate versus δ^2 under the different number of IRS elements. For the imperfect I-CSI case, the resource allocation, i.e., $\{p_{kj}, \tau_{kj}\}$, is first obtained based on the estimated I-CSI, i.e., $\hat{h}_{kj}$, which can be directly solved by our proposed algorithm. Then, we employ the obtained $\{p_{kj}, \tau_{kj}\}$ to calculate the sum-rate based on the real I-CSI, i.e., h_{kj}. From Fig. 6, it is expected that the ergodic sum-rate decreases with the increasing of δ^2. Moreover, one can observe that the ergodic sum-rate for $N = 80$ under the imperfect I-CSI even outperforms that for $N = 40$ under the perfect I-CSI, which indicates that the performance loss caused by imperfect I-CSI can be compensated by deploying more IRS reflecting elements.

Authorized licensed use limited to: Shanghai Jiaotong University. Downloaded on June 05,2023 at 08:45:12 UTC from IEEE Xplore. Restrictions apply.

V. Conclusion

In this paper, we proposed a novel two-timescale scheme to maximize the ergodic sum-rate in an IRS-aided energy-constrained IoT system employing DIBF. Specifically, multiple IRS BF patterns are first optimized based on the S-CSI, which varies much slowly than the I-CSI. With the optimized IRS BF patterns in each channel coherence interval, the resource allocation regarding the transmit powers and time allocations are optimized based on the effective I-CSI. The dimensional of the effective I-CSI is independent of the number of reflecting elements and thus the overhead of the I-CSI acquisition can be significantly reduced. To shed light on the fundamental performance-cost tradeoff, we analytically quantified the performance degradation incurred by using less IRS BF patterns. Simulation results verified the effectiveness of our proposed design and unveiled that only $K/3$ IRS BF patterns are needed for achieving the near-optimal performance in practice.

Appendix A
Proof of Theorem 1

To begin with, we first focus on the inner sum-rate maximization problem with respect to $\{\tau_{k\Omega(k)}\}$ in (8) under any given $\{\mathbf{\Theta}_j\}$ and $\{\Omega(k)\}$. The corresponding problem is written as

$$\max_{\{\tau_{k\Omega(k)}\}} \sum_{k=1}^{K} \tilde{R}_k \quad \text{s.t. (8b)}, \ \tau_{k\Omega(k)} \geq 0, \forall k. \tag{24}$$

It can be easily verified problem (24) is a convex optimization problem. By analyzing the Karush-Kuhn-Tucker (KKT) conditions of problem (24), we have

$$\frac{\left|h_{d,k} + \mathbf{h}_{r,k}^H \mathbf{\Theta}_{\Omega(k)} \mathbf{g}\right|^2}{\tau_{k\Omega(k)}^*} = \frac{\left|h_{d,l} + \mathbf{h}_{r,l}^H \mathbf{\Theta}_{\Omega(l)} \mathbf{g}\right|^2}{\tau_{l\Omega(l)}^*}, \forall k, l, \tag{25}$$

where $\{\tau_{k\Omega(k)}^*\}$ denotes the optimal solution for problem (24). Based on (25), the optimal value of problem (24) can be written in a closed-form expression as

$$\begin{aligned}\tilde{R} &= \sum_{k=1}^{K} \tau_{k\Omega(k)}^* \log_2\left(1 + E_{\max}\left|h_{d,k} + \mathbf{h}_{r,k}^H \mathbf{\Theta}_{\Omega(k)} \mathbf{g}\right|^2 / (\tau_{k\Omega(k)}^* \sigma^2)\right) \\ &= \sum_{k=1}^{K} \tau_{k\Omega(k)}^* \log_2\left(1 + \frac{\sum_{k=1}^{K} E_{\max}\left|h_{d,k} + \mathbf{h}_{r,k}^H \mathbf{\Theta}_{\Omega(k)} \mathbf{g}\right|^2}{\sum_{k=1}^{K} \tau_{k\Omega(k)}^* \sigma^2}\right) \\ &= T_c \log_2\left(1 + \sum_{k=1}^{K} E_{\max}\left|h_{d,k} + \mathbf{h}_{r,k}^H \mathbf{\Theta}_{\Omega(k)} \mathbf{g}\right|^2 / (T_c \sigma^2)\right).\end{aligned} \tag{26}$$

By applying the Jensen's inequality, the expectation of $\tilde{R}$ is upper bounded by

$$\mathbb{E}\left\{\tilde{R}\right\} \leq T_c \log_2\left(1 + \frac{\sum_{k=1}^{K} \mathbb{E}\left\{\left|h_{d,k} + \mathbf{h}_{r,k}^H \mathbf{\Theta}_{\Omega(k)} \mathbf{g}\right|^2\right\}}{E_{\max}^{-1} T_c \sigma^2}\right). \tag{27}$$

Then, we focus on the derivation of $\mathbb{E}\{|h_{d,k} + \mathbf{h}_{r,k}^H \mathbf{\Theta}_{\Omega(k)} \mathbf{g}|^2\}$. To this end, we have

$$z = \left|h_{d,k} + \mathbf{h}_{r,k}^H \mathbf{\Theta}_{\Omega(k)} \mathbf{g}\right|^2 = \left|\sqrt{\beta_k}\left(z_1 + z_2 + z_3 + z_4 + h_{d,k}\right)\right|^2, \tag{28}$$

where $z_1 = \sqrt{\gamma_g \gamma_k} \bar{\mathbf{h}}_{r,k}^H \mathbf{\Theta}_{\Omega(k)} \bar{\mathbf{g}}$, $z_2 = \sqrt{\gamma_g} \tilde{\mathbf{h}}_{r,k}^H \mathbf{\Theta}_{\Omega(k)} \bar{\mathbf{g}}$, $z_3 = \sqrt{\gamma_k} \bar{\mathbf{h}}_{r,k}^H \mathbf{\Theta}_{\Omega(k)} \tilde{\mathbf{g}}$, and $\beta_k = \rho_{r,k}^2 \rho_g^2 / ((\gamma_g + 1)(\gamma_k + 1))$. In (28), the first term z_1 is a deterministic component, and $\mathbb{E}\{z_m\} = 0$ for $m = 2, 3, 4$. Since $\tilde{\mathbf{h}}_{r,k}^H$, $\tilde{\mathbf{g}}$, and $h_{d,k}$ have zero means and are independent with each other, we can obtain

$$\mathbb{E}\left\{|z|^2\right\} = |z_1|^2 + \sum_{i=2}^{4} \mathbb{E}\left\{|z_i|^2\right\} + \rho_{d,k}^2, \tag{29}$$

where

$$\begin{aligned}\mathbb{E}\left\{|z_2|^2\right\} &= \gamma_g \mathrm{Tr}\left\{\bar{\mathbf{g}}^H \mathbf{\Theta}_{\Theta_{\Omega(k)}}^H \mathbb{E}\left\{\tilde{\mathbf{h}}_{r,k} \tilde{\mathbf{h}}_{r,k}^H\right\} \mathbf{\Theta}_{\Omega(k)} \bar{\mathbf{g}}\right\} \\ &= \gamma_g \mathrm{Tr}\left\{\bar{\mathbf{g}}^H \mathbf{\Theta}_{\Theta_{\Omega(k)}}^H \mathbf{\Theta}_{\Omega(k)} \bar{\mathbf{g}}\right\} = \gamma_g N,\end{aligned} \tag{30}$$

and $\mathbb{E}\{|z_3|^2\}$ and $\mathbb{E}\{|z_4|^2\}$ can be similarly derived as

$$\mathbb{E}\left\{|z_2|^2\right\} = \gamma_k N, \mathbb{E}\left\{|z_3|^2\right\} = N. \tag{31}$$

By applying (30) and (31) into (29), the proof is completed.

References

[1] M. DiRenzo et al., "Smart radio environments empowered by reconfigurable intelligent surfaces: How it works, state of research, and the road ahead," *IEEE J. Sel. Areas Commun.*, vol. 38, no. 11, pp. 2450–2525, Nov. 2020.

[2] Q. Wu and R. Zhang, "Beamforming optimization for wireless network aided by intelligent reflecting surface with discrete phase shifts," *IEEE Trans. Commun.*, vol. 68, no. 3, pp. 1838–1851, Mar. 2020.

[3] C. Pan et al., "An overview of signal processing techniques for RIS/IRS-aided wireless systems," in *Proc. IEEE J. Sel. Topics Signal Process.*, vol. 16, no. 5, pp. 883–917, Aug. 2022.

[4] B. Zheng, Q. Wu, and R. Zhang, "Intelligent reflecting surface-assisted multiple access with user pairing: NOMA or OMA," *IEEE Commun. Lett*, vol. 24, no. 4, pp. 753–757, Apr. 2020.

[5] X. Mu, Y. Liu, L. Guo, J. Lin, and N. Al-Dhahir, "Capacity and optimal resource allocation for IRS-assisted multi-user communication systems," *IEEE Trans. Commun.*, vol. 69, no. 6, pp. 3771–3786, Jun. 2021.

[6] B. Lyu, P. Ramezani, D. T. Hoang, S. Gong, Z. Yang, and A. Jamalipour, "Optimized energy and information relaying in self-sustainable IRS-empowered WPCN," *IEEE Trans.Commun.*, vol. 69, no. 1, pp. 619–633, Jan. 2021.

[7] Q. Wu, X. Zhou, W. Chen, J. Li, and X. Zhang, "IRS-aided WPCNs: A new optimization framework for dynamic IRS beamforming," *IEEE Trans. Wireless Commun.*, vol. 21, no. 7, pp. 4725–4739, Jul. 2022.

[8] Z. Chu, P. Xiao, M. Shojafar, D. Mi, J. Mao, and W. Hao, "Intelligent reflecting surface assisted mobile edge computing for Internet of Things," *IEEE Wireless Commun. Lett.*, vol. 10, no. 3, pp. 619–623, Mar. 2021.

[9] G. Chen, Q. Wu, W. Chen, D. W. K. Ng, and L. Hanzo, "IRS-aided wireless powered MEC systems: TDMA or NOMA for computation offloading?," *IEEE Trans. Wireless Commun.*, 2022, early access, Sep. 12, 2022, doi: 10.1109/TWC.2022.3203158.

[10] Y. Han, W. Tang, S. Jin, C.-K. Wen, and X. Ma, "Large intelligent surface-assisted wireless communication exploiting statistical CSI," *IEEE Trans. Veh. Technol.*, vol. 68, no. 8, pp. 8238–8242, Aug. 2019.

[11] M.-M. Zhao, Q. Wu, M.-J. Zhao, and R. Zhang, "Intelligent reflecting surface enhanced wireless networks: Two-timescale beamforming optimization," *IEEE Trans. Wireless Commun.*, vol. 20, no. 1, pp. 2–17, Jan. 2021.

[12] Q. Tao, S. Zhang, C. Zhong, W. Xu, H. Lin, and Z. Zhang, "Weighted sum-rate of intelligent reflecting surface aided multiuser downlink transmission with statistical CSI," *IEEE Trans. Wireless Commun.*, vol. 21, no. 7, pp. 4925–4937, Jul. 2022.

[13] K. Zhi, C. Pan, H. Ren, and K. Wang, "Statistical CSI-based design for reconfigurable intelligent surface-aided massive MIMO systems with direct links," *IEEE Wireless Commun. Lett.*, vol. 10, no. 5, pp. 1128–1132, May 2021.

[14] S. Abeywickrama, R. Zhang, Q. Wu, and C. Yuen, "Intelligent reflecting surface: Practical phase shift model and beamforming optimization," *IEEE Trans. Commun.*, vol. 68, no. 9, pp. 5849–5863, Sep. 2020.

[15] G. Zhou, C. Pan, H. Ren, K. Wang, and A. Nallanathan, "A framework of robust transmission design for IRS-aided MISO communications with imperfect cascaded channels," *IEEE Trans. Signal Process.*, vol. 68, pp. 5092–5106, 2020.

Authorized licensed use limited to: Shanghai Jiaotong University. Downloaded on June 05,2023 at 08:45:12 UTC from IEEE Xplore. Restrictions apply.